ELSEVIER

Biophysical Chemistry 128 (2007) 140–149

Biophysical Chemistry

http://www.elsevier.com/locate/biophyschem

Destabilised mutants of ubiquitin gain equal stability in crowded solutions

Andrew Roberts, Sophie E. Jackson *

Department of Chemistry, University of Cambridge, Lensfield Road, CB2 1EW, UK

Received 11 November 2006; received in revised form 16 March 2007; accepted 16 March 2007
Available online 30 March 2007

Abstract

This paper investigates the thermodynamic and kinetic response of WT* ubiquitin (F45W) and three mutants to high concentrations of glucose, sucrose and dextran under physiological temperature and pH. WT* ubiquitin was stabilised by the same amount when comparing each cosolute on a weight to volume ratio, with cosolute effects largely independent of denaturant concentration. The energy difference between the mutants and WT* ubiquitin also remained the same in high concentrations of cosolute. An apparent decrease in transition-state surface burial in the presence of the cosolutes was attributed to increased compaction of the denatured state, and not to the Hammond effect. Together, these results suggest higher thermodynamic stabilities and folding rates for proteins *in vivo* compared to *in vitro*, in addition to more compact denatured states. Because the effects of mutation are the same in dilute solution and crowded conditions used to mimic the cellular environment, there is validity in using measurements of mutant stabilities made in dilute solutions to inform on how the mutations may affect stability *in vivo*.

Keywords: Ubiquitin; Beta-Tanford value; Glucose; Protein folding; Denatured state

1. Introduction

Ubiquitin is a small, 76 residue β-grasp protein that has been extensively studied as a folding model for two decades [1]. Ubiquitin's amino acid sequence is 95% conserved from yeast to Man, with ubiquitin present in the cytosol of all eukaryotes. Ubiquitin selectively modifies the function of other proteins by covalent attachment through its C-terminus to exposed lysines on the target protein. Once linked through an iso-peptide bond to the target protein, further ubiquitins may be attached to lysines on the ubiquitin surface itself, forming ubiquitin chains recognised by a number of processes including protein degradation [2–5].

The intact ubiquitin fold is necessary for recognition of targeted proteins in endocytosis [6] and furthermore, a minimum concentration of ubiquitin is necessary for survival of cells after heat shock and other stress events [7,8]. Although cellular assays have probed the role of conserved residues exposed on the surface of ubiquitin, which are necessary for recognition of ubiquitin in a great many processes [6,9], the reason for the conservation of the hydrophobic core is still unknown.

Preservation of the recognition surface and the stability of ubiquitin are both likely reasons for its high sequence conservation. Although mutation of a handful of surface residues is conditionally lethal [6], the structure is remarkably resilient to core mutation, with the fold remaining intact when both overpacked and under-packed [10,11]. Experiments conducted on a F45W tryptophan mutant of ubiquitin, here referred to as the pseudo-wild type (WT*), revealed that hydrophobic-core mutations of WT* destabilise the protein, suggesting these residues might be conserved to maximise protein stability [12]. Therefore, it is likely that preserving the stability of ubiquitin, perhaps to maintain essential pools of the protein inside the cell, is the reason for the high conservation of the hydrophobic core.

Recent experiments to measure protein stability inside the cell have suggested that there are subtle differences between stability in dilute and crowded conditions, especially in the presence of organic osmolytes [13–15]. Because of the difficulty in measuring protein stability inside cells, many researchers have added both osmolytes and macromolecules at concentrations of 100–400 g/L to solutions *in vitro* to crowd the solution to the same degree as in the cell.

* Corresponding author. Tel.: +44 1223 762011.
E-mail address: sej13@cam.ac.uk (S.E. Jackson).
URL: http://www-jackson.ch.cam.ac.uk (S.E. Jackson).

0301-4622/$ - see front matter © 2007 Elsevier B.V. All rights reserved.
doi:10.1016/j.bpc.2007.03.011

In vitro experiments with carbohydrate-based macromolecules and osmolytes suggest that most proteins increase in stability with cosolute concentration in a linear, additive fashion [16,17], with typical increases in stability of around 1–2 kcal/mol in 200–300 g/L of cosolute [16,18–22]. These stability changes approximate those made by excluded volume theory, which estimates the change in stability of a protein on the basis of the difference between the compactness of the native and denatured states [23]. Minton predicts that crowding at around 300 g/L of cosolute should increase the equilibrium constant for folding by ten or a hundred times, or 1.4–2.8 kcal/mol for proteins at 310 K [23]. This prediction can be made because small, globular proteins undergo similar changes in compactness when unfolded, hence the small range of values obtained for a several different proteins.

Because single-point mutants of a protein should undergo almost identical changes in compaction during folding, excluded volume theory predicts the same absolute increase in stability for both the wild type and destabilised mutants at a fixed temperature in crowded solutions. Examination of destabilised mutants of ubiquitin here confirms this hypothesis, with an increase around 1.2 kcal/mol for WT*, I13A, K27A and I61V in 200 g/L glucose solution.

Independent from the excluded volume method for estimating stability gains in crowded solutions, a technique has been developed which uses the transfer free energies for solvent-exposed components of the protein to predict stability gains in the presence of osmolytes [24–27]. Although this technique is more specific to the protein examined than the excluded volume approach, it underestimates the stability gain of ubiquitin by 0.7 kcal/mol at 1 M sucrose, perhaps due to the concentration of charged and hydrophobic groups on the ubiquitin surface.

Proteins in crowded solutions display faster folding and slower unfolding, as anticipated from crowding theory [28]. Unexpectedly, both Silow and Russo [29,30], with CI2 and FKBP12, observed a decrease in the β_T value, suggesting an increase in surface exposure in the transition state, the opposite of what would be expected from crowding theory where more compact states are favoured [31]. Unfortunately, both proteins displayed kinetics that complicated an analysis of the decrease in β_T. FKBP12 had a slow refolding phase that refolded on a comparable timescale to prolyl isomerisation in the denatured state, complicating the relationship between the rate of refolding and denaturant concentration [32], while for CI2 the osmolyte, ethyleneglycol, changed the effective concentration of denaturant during kinetic experiments. CI2 also displayed premature collapse of the denatured state in response to crowding [29]. In this study, we have made similar measurements on ubiquitin where we do not have these complicating factors, revealing that the change in β_T is caused by changes in the denatured state in response to crowding.

This study suggests that excluded volume theory can be used to explain the same absolute change in stability observed for WT* and mutant ubiquitin in crowded conditions. Because the differences between mutant and wild-type stabilities are likely to be as large inside the cell as in dilute solution, these residues are perhaps conserved to maintain cellular ubiquitin levels.

2. Materials and methods

2.1. Materials

Analytical grade glucose, sucrose and dextran (average molecular weight 68,800 Da) were obtained from Sigma-Aldrich. Analytical-grade guanidinium hydrochloride (GdmCl), Isopropyl-thio-β-D-galactoside (IPTG), Tris HCl, Trizma base and ampicillin were obtained from Melford laboratories.

Pseudo-wild type F45W mammalian ubiquitin (WT*) was expressed from a pHisGroEL vector and purified as described previously [33]. Standard mutagenesis techniques (Stratagene) were used to introduce single point mutations into the WT* plasmid for construction of I13A, K27A and I61V mutants. All vectors were fully sequenced, and the purity of the protein assessed by SDS-PAGE and mass spectrometry. Protein concentration was calculated using a molar extinction coefficient, $\varepsilon_{280\ nm}$, of 6970 M^{-1} cm^{-1}.

2.2. General conditions

The WT*, two hydrophobic core mutants I13A and I61V and a charge mutant K27A were unfolded with GdmCl at 310 K, pH 7.4. With the exception of the increased temperature, these were the conditions established by Went as clearly being in the two-state regime for ubiquitin folding [33]. In all experiments, final buffer conditions were 50 mM Tris–HCl pH 7.4 at 310 K. Buffer and denaturant solutions were prepared as described elsewhere [34].

For the equilibrium experiments, final concentrations of ubiquitin were 2 μM and the experiments conducted as described by Main and coworkers [34]. Dextran solutions were dispensed by hand using a positive displacement pipette.

Kinetic experiments were performed using [GdmHCl]-jump experiments with a final protein concentration of 2 μM as described elsewhere [34].

Circular dichroism experiments were conducted on an Applied Photophysics Chirascan spectrometer at 37 °C, pH 7.4 with TrisCl buffer at 10 mM. The protein samples at 40 μM concentration were placed in a 1 mm quartz cuvette and spectra recorded at increments of 0.2 nm between 250 and 213 nm with a bandpass of 0.5 nm. The spectra were corrected for the buffer/denaturant and averaged over two runs.

2.3. Data fitting

2.3.1. Kinetic data

Unfolding traces were fitted to a single exponential process including linear drift to account for baseline instability when measurements were obtained over longer periods. Refolding traces were fitted to a triple-exponential process, with the multiple phases observed caused by heterogeneity in the unfolded state arising from proline isomerisation [35–37]. The major, fast refolding phase accounts for some 75% of the total change in signal, a slower phase accounts for some 20% with a rate constant some 15-fold slower than the fast phase, and a small (5%) very slow phase has a rate constant 4000-fold slower than the fast

phase [35]. Krantz and Sosnick have shown that the same refolding rate constants for the fast phase are obtained using either single-jump experiments (in which proline-isomerisation phases are present) or double-jump experiments (in which no proline-isomerisation phases are present) [38]. Thus, the fast phase is well resolved from the slower phases and the kinetic traces can be fit to multi-exponential functions to obtain accurate rate constants for the major folding phase. It should be noted that the Searle group has recently shown that the slow phases observed for the folding of an engineered variant of yeast ubiquitin may be attributed to the formation of an on-pathway intermediate [39], at the present time, there is no evidence for this intermediate with mammalian ubiquitin ([35–38] and the two-state model is therefore used here.

Kinetic data were fitted to a two-state folding model using the following equation [40]:

$$\ln k = (k_F^{H_2O}\exp(-m_{k_F}[D]) + k_U^{H_2O}\exp(+m_{k_U}[D])) \quad (1)$$

where $k_F^{H_2O}$ and $k_U^{H_2O}$ are the rate constants for folding and unfolding in water, respectively, [D] the concentration of denaturant and m_{k_F} and m_{k_U} the slopes of the refolding and unfolding arms of the Chevron plot, respectively.

The effect of the addition of cosolute on the activation energy barrier to unfolding, defined as the energy change between the native state and transition state for the protein in the presence and absence of cosolute, $\Delta\Delta G_{TS\text{-}F}$, is calculated by:

$$\Delta\Delta G_{TS-F} = -RT\ln(k_U/k_U') \quad (2)$$

where k_U and k_U' are the rate constants of unfolding for the protein in denaturant and protein at the same concentration of denaturant in solution with the cosolute, respectively. Similarly, the effect of cosolute on the activation energy barrier to folding, $\Delta\Delta G_{U\text{-}TS}$, is given by:

$$\Delta\Delta G_{U-TS} = RT\ln(k_F/k_F') \quad (3)$$

where k_F and k_F' are the rate constants for refolding for the protein and protein in solution with cosolute, respectively. Kinetic m-values for the sensitivity of the folding ($m_{U\text{-}TS}$) and unfolding ($m_{TS\text{-}F}$) reactions were obtained from the respective slopes of the folding (m_{k_F}) and unfolding (m_{k_U}) arms of the chevron plots multiplied by RT.

β_T-values, representing the fraction of surface burial of the transition state relative to the native state, were calculated from the kinetic m values using:

$$\beta_T = m_{k_F}/(m_{k_F} + m_{k_U}) \quad (4)$$

Hammond behaviour is analysed as described elsewhere [41].

2.3.2. Equilibrium data

The fluorescence intensities, F, obtained from the equilibrium unfolding experiment were fitted to the equation below [42].

$$F = \frac{(\alpha_N + \beta_N[D]) + (\alpha_U)\exp((m_{U-F}[D] - \Delta G_{U-F}^{H_2O})/RT)}{1 + \exp((m_{U-F}[D] - \Delta G_{U-F}^{H_2O})/RT)} \quad (5)$$

where α_N and β_N are the intercept and slope of the low denaturant baseline, [D] the concentration of denaturant, α_U the intercept of the high denaturant baseline, $m_{U\text{-}F}$ the linear dependence of the free energy of unfolding on denaturant concentration and $\Delta G_{U\text{-}F}^{H_2O}$ is the equilibrium free energy of unfolding in water.

The change in equilibrium unfolding energy of the mutants in the presence of cosolutes compared to that in the absence of cosolutes, $\Delta\Delta G_{U\text{-}F}^{trs}$, is given by the equation:

$$\Delta\Delta G_{U-F}^{trs} = \Delta G_{U-F}^{[cosolute]} - \Delta G_{U-F}^{H_2O} \quad (6)$$

where $\Delta G_{U\text{-}F}^{[cosolute]}$ is the free energy of unfolding of the protein in a particular concentration of cosolute.

2.3.3. Test for native-state aggregation

To ensure that any change in equilibrium stability was not caused by aggregation of the native state, WT* at 2 μM, pH 7.4 and 37 °C was equilibrated for 24 h in 300 g/L glucose. Light scattering at 90° to the incident beam [19] was monitored at six different excitation–emission wavelengths between 320 and 520 nm using an Aminco Bowman UV–vis spectrometer and no change in scattering intensity was observed (data not shown). It was concluded that no appreciable aggregation of the native state of WT* occurred in concentrations up to 300 g/L glucose.

2.4. Test for independence of glucose and denaturant effects

The method of Jourdan and Searle [17] was followed to test for the independence of the effects of glucose and GdmCl on the WT*. If glucose and GdmCl act on the protein in an additive manner, the values for the midpoint in glucose, or $[D]_{(50\%)}$ of the protein would fit the equation:

$$[D]_{50\%} = \frac{-m_{U-F}^2}{m_{U-F}^1}[\text{glucose}] + \frac{\Delta G_{U-F}^{H_2O}}{m_{U-F}^1} \quad (7)$$

where [glucose] is the concentration of glucose and $m_{U\text{-}F}^1$ and $m_{U\text{-}F}^2$ are the linear dependencies of the free energy of unfolding on denaturant and glucose concentration, respectively.

2.5. Estimation of the free energies of transfer to sucrose solution

The calculation of group transfer free energies for ubiquitin into sucrose solution was conducted as described elsewhere [26,27] using values for the transfer free energies of the side chains and backbone obtained from [24]. The solvent accessible surface area for ubiquitin was calculated from atomic coordinates in the 1UBQ structure deposited at the Protein Data Bank at Brookhaven using Marc Gerstein's calc-surface program [43] and a probe of radius 1.4 Å. The N-terminal tag on WT* was assumed to be unstructured in the native state and the surface area of the tryptophan introduced at position 45 was assumed to be exposed to the same degree as the phenylalanine in the 1UBQ structure.

3. Equilibrium unfolding

Three sets of equilibrium unfolding curves were measured for WT* and the three destabilised mutants of ubiquitin under physiological-like conditions. First, the stabilities were measured at 37 °C, and then two different types of crowding agent were used to mimic the environment within the cell — one small molecule, glucose and a larger polymer, dextran. Results are shown in Fig. 1 and the thermodynamic parameters summarised in Tables 1 and 2. The stability of WT* and the mutant ubiquitins was not significantly different at 37 °C compared to previously published results at 25 °C, as can be seen from Table 1 and [12].

A slight decrease in stability of 0.3±0.4 kcal/mol for WT* was observed in 50 g/L of both glucose and dextran solutions. These unexpected decreases were within error, yet repeatable. The decrease in stability in low concentrations of glucose may be caused by an artefact, a relative increase in residual structure in the denatured state or perhaps due to removal of stabilising Cl^- interactions between the protein and the denaturant. Previous studies [44] suggested that Cl^- ions bind to ubiquitin and stabilise the native state, and this interaction could be removed when addition of glucose forces preferential hydration of the protein surface [45]. Examination of I13A, K27A and I61A in 50 g/L glucose did not reveal a similar decrease in stability for these destabilised mutants (Table 1), suggesting this effect may be limited to the WT* only, and not caused by the presence of Cl^- ions. Furthermore, circular dichroism spectra in the far-UV of WT* in 50 g/L glucose did not show any perceptible change in conformation in either the native or denatured states (data not shown), suggesting it is unlikely to be caused by a ground-state conformational change of WT*. Given that the result for WT* was also not observed in the kinetic analysis, we do not think this apparent destabilisation in low quantities of crowding agent is significant.

Interestingly, the stabilisation of the mutants was comparable in dextran or glucose, even though dextran is significantly larger in size than glucose. This suggests ubiquitin stability increases in polyol solution may be determined principally by the density of the polyol solution, and not altered significantly by the molecular weight of the polyol.

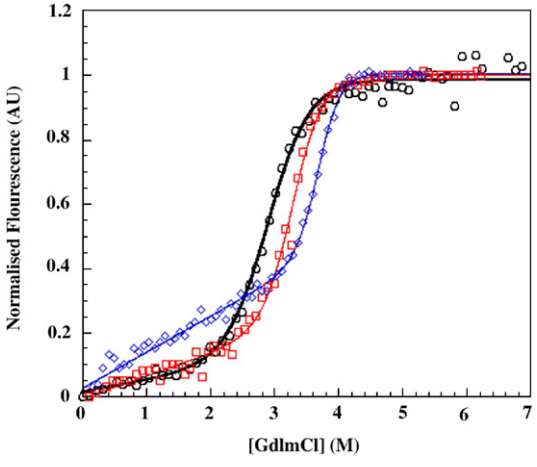

Fig. 1. Representative equilibrium unfolding curves for WT* ubiquitin at 310 K, pH 7.4 with GdmCl as the denaturant. Black=0 g/L, red=150 g/L and blue=300 g/L glucose. (For interpretation of the references to colour in this figure legend, the reader is referred to the web version of this article.)

Table 1
Ubiquitin stability as a function of glucose concentration at pH 7.4, 37 °C

Mutant	Glucose concentration (g/L)	$[GdmCl]_{50\%}$ (M)	$m_{U\text{-}F}$ (kcal/mol M)	$\Delta G_{U\text{-}F}^{H_2O}$ (kcal/mol)	$\Delta\Delta G_{U\text{-}F}^{trs}$ (kcal/mol)
WT*	0	2.87±0.02	2.5±0.13	6.1±0.3	–
	50	2.69±0.010	3.1±0.11	5.8±0.3	−0.3±0.4
	50	2.65±0.012	3.1±0.13	5.7±0.3	−0.4±0.4
	100	2.90±0.02	3.2±0.25	6.2±0.3	0.1±0.4
	150	3.27±0.01	2.7±0.10	7.0±0.4	0.9±0.6
	200	3.59±0.02	2.2±0.10	7.7±0.4	1.6±0.6
	250	3.54±0.02	2.3±0.1	7.6±0.4	1.5±0.6
	300	3.71±0.01	3.2±0.2	7.9±0.4	1.8±0.6
I13A	0	1.33±0.03	2.5±0.14	2.8±0.2	–
	50	1.43±0.02	2.6±0.10	3.05±0.2	0.3±0.3
	200	1.75±0.010	3.5±0.11	3.7±0.2	0.9±0.3
K27A	0	1.61±0.04	2.5±0.2	3.4±0.2	–
	50	2.04±0.05	2.7±0.3	4.4±0.2	1.0±0.3
	200	2.13±0.010	3.1±0.11	4.6±0.2	1.2±0.3
I61V	0	2.24±0.04	2.5±0.3	4.8±0.5	–
	50	2.53±0.02	2.5±0.18	5.4±0.3	0.6±0.6
	200	2.96±0.02	2.7±0.2	6.3±0.3	1.5±0.6

$\Delta G_{U\text{-}F}^{H_2O}$ is calculated using an $\langle m_{U\text{-}F}\rangle$ value of 2.14±0.11 kcal/mol M obtained from the average kinetic $m_{U\text{-}F}$ for all data, and the free energy calculations are compared to each mutant in 0 g/L glucose.

The increase in stability of WT* in concentrations of dextran and glucose over 50 g/L appears to be linear with cosolute concentration (Fig. 2), suggesting that an *m*-value for the sensitivity of equilibrium unfolding to glucose could be calculated for WT* similar to that obtained for GdmCl. To examine if the effects of glucose/dextran and GdmCl are separable, allowing such an *m*-value to be calculated, the data for glucose was analysed using the technique established for ubiquitin and methanol by Jourdan and coworkers [17].

4. Additive effects of glucose and denaturant

If the denaturant and glucose act independently on ubiquitin stability, the intercept of $[D]_{50\%}$ versus [glucose], $\Delta G_{U\text{-}F}^{H_2O}$, should equal the value for the $[D]_{50\%}$ of WT* in the absence of glucose. The plot below in Fig. 2 has an intercept on the *y*-axis of 2.64±0.10 M, fractionally below the expected value of 2.87±0.01 M. Furthermore, the gradient of the linear fit should

Table 2
Ubiquitin stability in dextran solution, pH 7.4, 37 °C

Mutant	[Dextran] (g/L)	$[GdmCl]_{50\%}$ (M)	$m_{U\text{-}F}$ (kcal/mol M)	$\Delta G_{U\text{-}F}^{H_2O}$ (kcal/mol)	$\Delta\Delta G_{U\text{-}F}^{trs}$ (kcal/mol)
WT*	0	2.87±0.01	2.5±0.1	6.1±0.3	–
	50	2.71±0.01	3.0±0.1	5.8±0.3	−0.3±0.4
	100	3.22±0.03	2.6±0.03	6.9±0.4	0.8±0.5
	150	3.4±0.07	2.3±0.4	7.3±0.4	1.2±0.5
I13A	0	1.33±0.03	2.7±0.13	2.8±0.2	–
	100	1.57±0.14	2.6±0.8	3.4±0.3	0.6±0.4
K27A	0	1.62±0.03	2.5±0.2	3.4±0.2	–
	100	1.78±0.10	3±1.0	3.8±0.3	0.4±0.4
I61V	0	2.24±0.04	2.5±0.1	6.1±0.3	–
	100	2.69±0.06	2.4±0.4	5.8±0.3	1.0±0.4

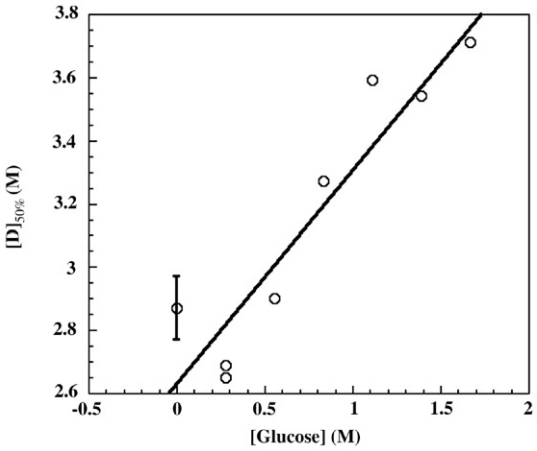

Fig. 2. The change in the midpoint of denaturation of WT* with glucose concentration. The relationship is linear and suggests the stabilising effect of glucose (and dextran as they show the same trend) is separable from the denaturing effect of GdmCl. $R=0.93$.

equal the ratio of the two *m*-values for glucose and denaturant. Substituting in the denaturant $m^1_{U\text{-}F}$-value of 2.14 kcal/mol M obtains an $m^2_{U\text{-}F}$-value for glucose of -1.4 ± 0.2 kcal/mol M. The linear dependence of the stability of WT* on glucose concentration is smaller than that of GdmCl and opposite in sign, indicating that glucose stabilises the protein.

The discrepancy between the *y*-intercept in Fig. 2 and actual midpoint of denaturation suggests that we cannot be certain that the denaturant and cosolute effects are independent, however the difference is sufficiently small that stability predictions of WT* in higher concentrations of glucose should be fairly accurate.

5. Estimation of the free energy of transfer to sucrose

An independent method for estimating the stability gain in sucrose (but not yet glucose) solution has been provided by Bolen and coworkers [26,27]. Using the free energy of transfer for exposed sections of the peptide backbone and side-chains, Bolen and coworkers calculated the sum of the free energy change for both the native and averaged denatured states when placed in sucrose solution. The difference, when measured at 1 M concentration of sucrose, is the $m^2_{U\text{-}F}$-value for the effect of sucrose on the unfolding free energy of the protein.

The approach documented by Auton and Bolen was followed here for ubiquitin as it had previously been followed for RCAM-T1, the T62P mutant of staphylococcal nuclease and the protein component of RNase P [27]. The results for WT* ubiquitin are shown in Table 3. Actual values for sucrose solution were obtained experimentally and are presented for comparison.

From the data presented in Table 3 it can be seen that transfer of ubiquitin's peptide backbone to sucrose solution is highly unfavourable and is the main contributor to increased stability in sucrose solution, in agreement with the findings of Liu and coworkers [24]. In contrast, transfer of the side-chains for both the native and denatured states to sucrose is favourable. Side-chain transfer is not, however, sufficient to overcome the unfavourable transfer of the backbone, as observed with several other group transfer calculations [25,24,27].

Closer inspection of Table 3 reveals transfer of native ubiquitin to 0.5 M sucrose is slightly unfavourable by 0.08 kcal/mol, a result not anticipated from the previous studies and contradictory to the favourable transfer of the native state to 1 M sucrose. It is possible, therefore, that small amounts of cosolute may destabilise the native state slightly, producing the non-additive effects seen for WT* in 50 g/L glucose.

The calculated free energy changes for the WT* do not agree well with the experimental values in sucrose for either the minimum or maximum estimates of the denatured state solvent accessible surface area (Table 3). Values are significantly below the 1.4 and 2 kcal/mol found experimentally. The approximation of the denatured state using the data in Creamer's method [46] is unlikely to be the source of the difference between calculated and measured transfer free energies, because even using values for the total accessible surface area [47] for the denatured state (that is without any surface burial whatsoever) still underestimates the transfer free energies by 0.2 and 0.6 kcal/mol for 0.5 and 1 M sucrose, respectively (data not shown).

The discrepancy between calculated and expected values for the stabilising effect could be caused by the grouping of similar side-chains together on the surface of ubiquitin. Ubiquitin has a hydrophobic stripe based on three residues that are involved in the recognition of ubiquitin-tagged proteins by the proteasome [48]. This stripe is surrounded by five positively charged residues [49], and this electrostatic cluster may interact with osmolytes in a manner not accounted for by a simple additive transfer free energy calculation [50]. Binding of sucrose to this site in the native conformation could create additional stability not included in the simple group transfer calculation. Comparison of the ubiquitin data with the data collected by Auton [27] on several other proteins suggests that although group transfer calculations tend to underestimate experimental values, the magnitude of the discrepancy with ubiquitin is too large to consider the values in agreement.

Table 3
Estimated transfer energies of ubiquitin to sucrose solution calculated using the group transfer free energies of solvent accessible surfaces of WT* ubiquitin

	[Sucrose] (M)	Side chain ΔG^{trs} (cal/mol)	Backbone ΔG^{trs} (cal/mol)	Total ΔG^{trs} (cal/mol)	$\Delta\Delta G^{trs}_{U\text{-}F}$ (kcal/mol)
Native	1	−541	353	−188	–
Denat. (max)	1	−600	1654	1054	1.24
Denat. (av)	1	−551	1310	759	0.95
Denat. (min)	1	−501	966	465	0.65
Native	0.5	−170	251	80	–
Denat. (max)	0.5	−190	1175	985	1.07
Denat. (av)	0.5	−175	931	756	0.68
Denat. (min)	0.5	−159	687	528	0.45
Experimental	0.5	–	–	–	1.4±0.4
Experimental	1	–	–	–	2.0±0.4

Actual experimental values are given for comparison.

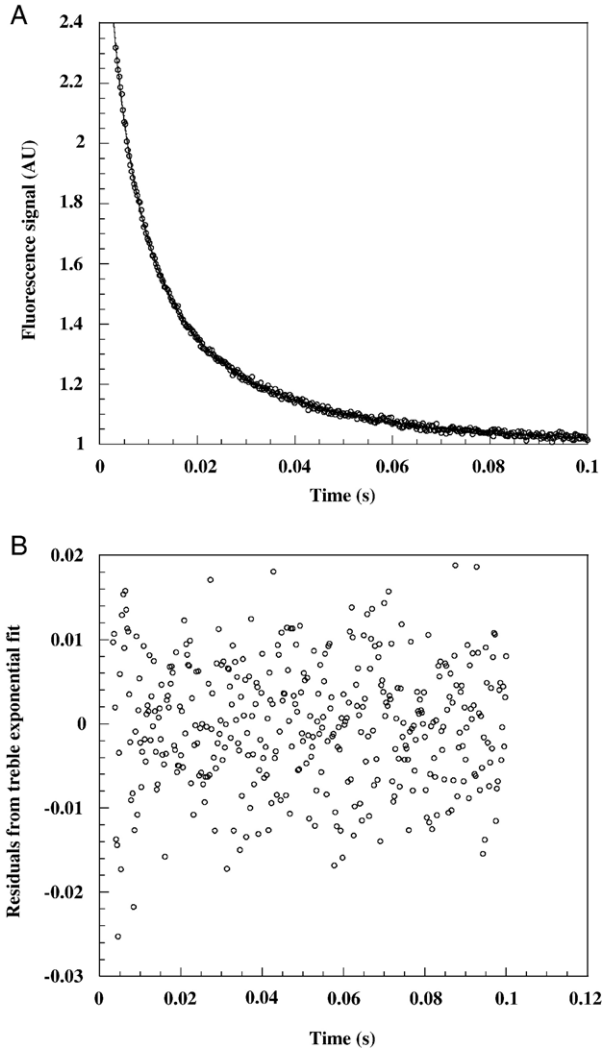

Fig. 3. WT* refolding into buffer containing 100 g/L glucose as monitored by tryptophan fluorescence at 353 nm (A). The data fits well to a triple exponential as can be seen by the random residual distribution about zero (B).

5.1. Equilibrium unfolding in sucrose

Comparing the experimental results for sucrose (Table 3) with the results for glucose (Fig. 2) shows sucrose to be the stronger stabilising agent by 0.7 and 0.6 kcal/mol at 0.5 and 1 M concentrations, respectively. This relationship was expected from previous studies on other proteins [16,21]. Comparing values at fixed densities of solute suggests that the increases in WT* stability in glucose and sucrose are within error, as they were when comparing glucose to dextran at the same concentration (Table 2). These findings suggest glucose, sucrose and dextran are equally good stabilising agents at a given density of polyol solution, perhaps because they are similar enough in chemical identity that the common soft interactions and excluded volume effect are the same for each cosolute.

6. Kinetic results

Kinetic data for folding and unfolding of the four mutants was collected by stopped-flow fluorescence spectroscopy and a typical trace is presented in Fig. 3. Plotting the logarithm of the observed folding/unfolding rate constants against denaturant concentration yielded chevron plots consistent with two-state folding [40] as shown for the pseudo-wild type in Fig. 4.

The slight (0.3±0.4 kcal/mol) destabilisation at 50 g/L observed in the equilibrium experiments for WT* ubiquitin was not observed in the kinetic experiments (Table 4). The kinetic $\Delta\Delta G_{\text{U-F}}$ was calculated from extrapolation of the unfolding rate to 0 M denaturant. Errors inherent in this extrapolation often create misleading rate constants for unfolding, so the rate constant for unfolding, k_{U}, was taken at 5 M GdmCl for WT* in 50 g/L glucose (data not shown). These values were still stabilising at 0.3±0.12 kcal/mol, suggesting that small quantities of glucose are unlikely to destabilise ubiquitin.

The folding rate constant increased and unfolding rate constant decreased in glucose in a manner expected from increased equilibrium stability. These effects agree with those observed with other proteins [30,29] and fit closely to the observed trend in $\Delta G_{\text{U-F}}^{\text{H2O}}$ from equilibrium stabilities. Interestingly, the folding rate constant for WT* appears to increase only to around 2000 s^{-1} (Table 4), which may be the maximum increase possible for glucose-assisted refolding.

Stopped-flow fluorescence spectrometry of the four mutants in dextran solutions was also conducted, but signal scattering at concentrations above 100 g/L and the generally high viscosity of the dextran solution created large fitting errors. Furthermore, no apparent increase in stability of the four mutants was observed in 100 g/L dextran solution, as tabulated in Table 5. Analysis of the kinetics data obtained in dextran solution is therefore difficult, with the refolding and unfolding rate constants k_{F} and k_{U} unchanged within error from those in dilute solution.

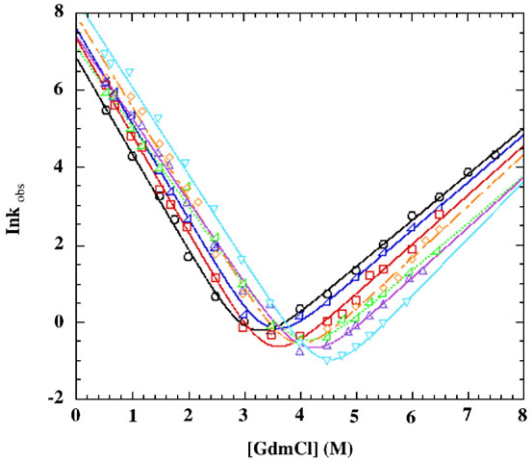

Fig. 4. A compilation of chevron plots for WT* fitted to the two-state folding equation Eq. (1). These depict the observed rate constants for folding and unfolding for the pseudo-wild type in 0 (black), 50 (navy dashed), 100 (red), 150 (green dotted), 200 (orange dashed), 250 (purple) and 300 (sky blue) g/L of glucose. (For interpretation of the references to colour in this figure legend, the reader is referred to the web version of this article.)

Table 4
Folding and unfolding kinetic parameters from data collected at pH 7.4, 37 °C with GdmCl as a denaturant

	[Glucose] (g/L)	$k_F^{H_2O}$ (s^{-1})	m_{k_F} (M^{-1})	$k_U^{H_2O}$ (s^{-1})	m_{k_U} (M^{-1})	$\Delta\Delta G_{TS\text{-}F}$ (kcal/mol)	$\Delta\Delta G_{U\text{-}TS}$ (kcal/mol)	$\Delta\Delta G_{U\text{-}F}^{kin,trs}$ (kcal/mol)
WT*	0	931±105	2.48±0.05	0.011±0.002	1.20±0.03	–	–	–
	50	2034±300	2.46±0.07	0.0064±0.003	1.24±0.08	−0.33±0.15	0.48±0.08	0.81±0.17
	100	1572±200	2.51±0.07	0.0034±0.0014	1.27±0.07	−0.72±0.3	0.32±0.05	1.0±0.3
	150	1680±200	2.15±0.05	0.0027±0.0014	1.21±0.09	−0.86±0.5	0.36±0.06	1.2±0.5
	200	2162±400	2.24±0.11	0.0016±0.0014	1.35±0.17	−1.19±1.1	0.51±0.1	1.7±1.1
	250	1664±200	2.13±0.06	0.0012±0.0008	1.30±0.12	−1.36±0.9	0.35±0.06	1.7±0.9
	300	2095±400	2.01±0.08	0.0006±0.0001	1.66±0.4	−1.84±0.5	0.5±0.11	2.3±0.5
I13A	0	134±50	3.5±0.5	0.56±0.09	0.88±0.03	–	–	–
	200	339±26	2.78±0.07	0.20±0.02	0.91±0.02	−0.63±0.19	0.6±0.4	1.2±0.4
K27A	0	954±324	2.54±0.32	1.9±0.7	0.78±0.06	–	–	–
	200	1510±381	2.10±0.17	0.36±0.19	0.95±0.10	−1.0±0.6	0.3±0.4	1.3±0.7
I61V	0	1102±161	2.62±0.01	0.041±0.010	1.20±0.04	–	–	–
	200	2342±419	2.28±0.10	0.008±0.004	1.30±0.09	−1.0±0.7	0.5±0.2	1.5±0.7

Data fitted well to the two-state folding equation, generating the values in the Table above. The free energy calculations are relative to each mutant in 0 g/L glucose.

6.1. Movement of the denatured state along the reaction coordinate

The kinetic parameters in Table 4 suggest that the transition state becomes less compact as the concentration of glucose is increased (β_T is decreasing in the presence of glucose). Similar decreases in the β_T value were observed by Russo and coworkers and Silow and coworkers with FKBP12 and CI2 in TMAO and ethyleneglycol [30,29]. Neither team of researchers offered an explanation for the decrease in β_T value which represents an increase in solvent accessible surface area in the transition state, the opposite of what might be expected in a crowded solution favouring more compact states [51].

A possible explanation would be Hammond behaviour, where the protein shifts its transition state along the reaction coordinate towards the ground state that is destabilised by a perturbation [52]. In the case of adding cosolutes that stabilise the native state compared to the denatured state (as can be seen with $\Delta\Delta G_{TS\text{-}F}$ and $\Delta\Delta G_{U\text{-}TS}$ in Table 4), Hammond behaviour would occur as movement in the position of the transition state towards the denatured state. Fig. 5 shows movement of the β_T-value towards the denatured state with an increasing activation energy barrier to unfolding, suggesting Hammond-like behaviour.

It is, however, possible to postulate that such behaviour in response to stabilising cosolutes could be explained by structural changes of the ground states [53], a switch between parallel pathways [54] or change in rate limiting step during folding [54]. These can be considered in turn.

Examination of the cross-interaction parameter [55] for the data suggests it is close to zero, but positive (data not shown). Positive cross-interaction parameters indicate the absence of parallel pathways for folding [55]. Although parallel folding pathways have been suggested for yeast sequence ubiquitin [39], studies in the Jackson laboratory have not suggested parallel pathways exist for mammalian ubiquitin, and Ψ-value transition state analysis suggests a single pathway is traversed in the transition-state ensemble [56]. The rate-limiting step for refolding of two-state proteins is collapse of the denatured state [38], and a change in rate-limiting step would manifest itself as premature collapse of the coil as observed with CI2 [29]. This would be observable as a rollover on the refolding arm of the chevron plot, which was not observed for ubiquitin, suggesting that the rate-limiting step is not changing. This leaves structural changes in the ground states as possible explanation for the apparent Hammond behaviour.

$m_{U\text{-}TS}$ (but not $m_{TS\text{-}F}$) increases with $m_{U\text{-}F}$ (Table 4 and Fig. 6), suggesting that the difference in surface burial between the native and transition states remains constant, whilst the relative surface burial of the denatured state increases with added glucose (Fig. 6). Apparent movement in the position of the transition state relative to the ground states, falsely attributed to Hammond behaviour [55], also failed to show any increase in $m_{TS\text{-}F}$ with $m_{U\text{-}F}$. Furthermore, a comparison of far-UV CD data for WT* in 6 M GdmCl with and without 300 g/L glucose present (Fig. 7) suggests that there is slightly more secondary structure in the denatured state of ubiquitin in the presence of glucose, indicating

Table 5
Kinetic data for WT* and the mutants in dextran at pH 7.4, 37 °C

Mutant	[dextran] (g/L)	$k_F^{H_2O}$ (s^{-1})	m_{k_F} (M^{-1})	$k_U^{H_2O}$ (s^{-1})	m_{k_U} (M^{-1})	$m_{U\text{-}F}^{kin}$ (kcal/mol M)	$\Delta G_{U\text{-}F}^{kin}$ (kcal/mol)	β_T
WT*	0	931±10	2.48±0.05	0.011±0.002	1.2±0.03	2.26±0.07	7.0±1.3	0.67±0.06
	100	1045±100	2.47±0.07	0.013±0.004	1.17±0.06	2.24±0.13	7.0±2.3	0.68±0.09
I13A	0	134±50	3.29±0.52	0.56±0.09	0.88±0.03	2.6±0.4	3.4±1.4	0.8±0.5
	100	143±50	3.3±0.3	0.45±0.09	0.91±0.04	2.6±0.3	3.5±1.4	0.78±0.3
K27A	0	954±300	2.54±0.32	1.92±0.65	0.78±0.06	2.0±0.3	3.8±1.8	0.77±0.3
	100	950±200	2.54±0.15	1.55±0.28	0.83±0.04	2.1±0.15	3.9±1.1	0.75±0.16
I61V	0	1102±200	2.62±0.01	0.041±0.010	1.20±0.04	2.35±0.08	6.3±0.3	0.69±0.04
	100	1648±500	2.70±0.21	0.016±0.012	1.35±0.20	2.5±0.4	7.1±4.6	0.67±0.3

Change in both folding and unfolding rate constants was within error of values obtained in the absence of dextran. The errors are large due to scattering of the fluorescence signal in the stopped-flow instrument.

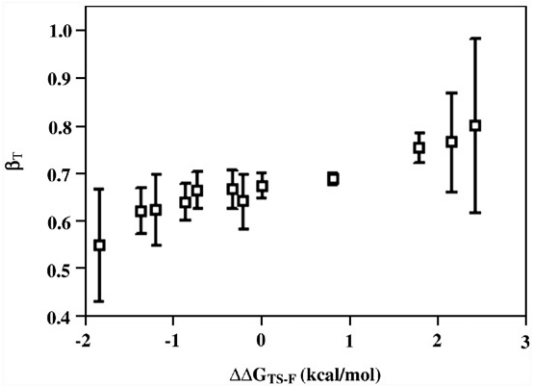

Fig. 5. Pseudo-Hammond behaviour of the WT* and mutants represented by movement of the β_T-value with the barrier to unfolding, $\Delta\Delta G_{TS\text{-}F}$.

a more compact denatured state. This suggests that only the denatured state of ubiquitin changes its position on the reaction coordinate when glucose is added to solution.

It appears, therefore, that ubiquitin experiences a compaction of the denatured state in glucose solution and not Hammond behaviour. Compaction of the denatured state is a prediction of macromolecular crowding theory [23] and compaction of denatured [57] and native [58] states has been observed experimentally. However, no collapse was observed for rapid transfer of unfolded ubiquitin to native conditions by small-angle X-ray scattering in the absence of crowding agent [59], suggesting that glucose is required to promote partial collapse of the denatured state of ubiquitin.

Thus, the decrease in β_T with added glucose, which suggested an expansion of the transition state is in fact caused by increased surface burial of the denatured state. The kinetic *m*-values of Russo and coworkers follow the same pattern as those obtained in this study with ubiquitin, suggesting similar compaction for FKBP12, although further studies are required to confirm this hypothesis.

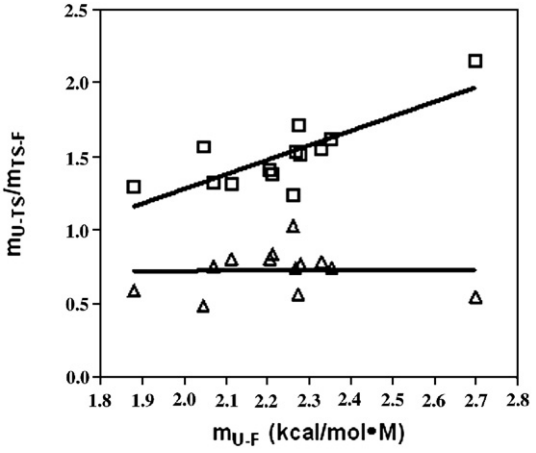

Fig. 6. The sensitivities of the folding (squares) and unfolding (triangles) reactions of WT*, I13A, K27A and I61A to denaturant compared to their equilibrium sensitivities in concentrations of glucose between 0 and 300 g/L. The only significant increase is observed for the folding reaction, indicating a narrowing of the gap between the denatured and transition states on the reaction coordinate.

7. Discussion

Ubiquitin, like CI2 [20,29], FKBP12 [30,60], lysozyme [22,61,62], ferri-cytochrome *C* [22,21] and several other proteins increases its stability in solutions containing both small osmolytes and larger macromolecules. The equilibrium free energy of unfolding for ubiquitin WT* and the three mutants I13A, K27A and I61V increased by around 1.3 ±0.4 kcal/mol in the presence of 200 g/L of glucose, a value consistent with other proteins in solutions containing polyols.

If the primary interaction stabilising ubiquitin in crowded solution was from steric repulsion caused by the polyol [16], we would expect that the increase in stability of the protein would be the same for all the mutants and additive to the effects of the denaturant. This appears to be the case for the mutants as they are all stabilised to the same extent.

The linear increase in ubiquitin stability observed with cosolute concentration is similar to that seen for ubiquitin in methanol [17], suggesting glucose acts on WT* stability in an additive fashion. This relationship brakes down, however, at low concentrations of glucose and dextran. Destabilising structural changes in the ground states could be the cause of non-additivity, however, far-UV CD analysis did not indicate any changes in structure in either the native or denatured states of WT* (data not shown). Furthermore, examination of the mutants at 50 g/L did not show any appreciable destabilisation, suggesting binding of denaturant anions [44] or soft interactions between the protein and cosolute [63] are unlikely to be the source of this discrepancy because they would appear equally for all the mutants. Ladurner and coworkers [20] observed a similar decrease in stability of CI2 in 50 g/L of povidone solution, indicating small amounts of cosolute can destabilise proteins, although the mechanism requires further investigation. Still, the effects of glucose were additive enough that it is possible to estimate the increase in WT* or mutant stability in concentrations from 100 to 300 g/L of glucose.

We have established that present techniques for estimation of the transfer free energy for ubiquitin cannot be applied with

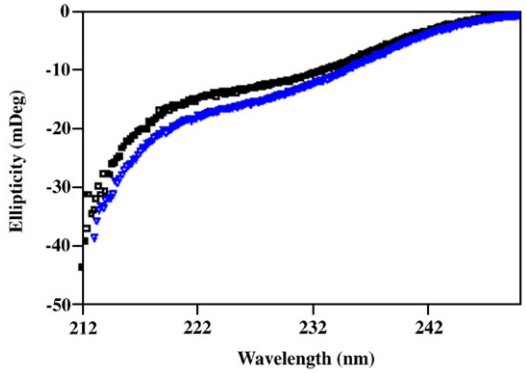

Fig. 7. Circular dichroism spectra for denatured WT* at 40 μM in the presence (blue triangles) and absence (black squares) of 300 g/L glucose, baseline corrected. There is a small increase in secondary structure when glucose is present as indicated by more negative ellipticity at wavelengths between 230 and 215 nm. (For interpretation of the references to colour in this figure legend, the reader is referred to the web version of this article.)

certainty. Comparison of equilibrium unfolding data for WT* in sucrose with values calculated using the transfer free energy approach developed by Bolen and coworkers [27,25,24] suggested that this approach underestimates the actual gain in stability for ubiquitin by 0.7 kcal/mol at 1 M sucrose. This is considerably more than the previous discrepancy for RCAM RNase [27] of under 0.4 kcal/mol. The most likely reason for the size of this discrepancy is the presence of localised charges on the surface of ubiquitin [49] interfering with the additivity of the group transfer calculation [50]. Inclusion of these effects in future models could yield better predictions for ubiquitin stability in crowded solutions.

Kinetic analysis of WT* and the three mutants all showed two-state behaviour under the experimental conditions in up to 300 g/L of crowding agent. Unlike in other experiments [30,62,20], the rate constant of refolding reached a maximum for all the mutants at around 2000 s^{-1}. This could represent the maximum refolding rate achievable for ubiquitin under physiological conditions, or it could be a consequence of changes in the denatured state caused by addition of glucose. It may also be that folding is becoming limited by viscosity under the conditions used, that is, conditions of high macromolecular crowding.

Closer analysis of the m_{k_F}- and m_{k_U}-values, alongside the far-UV CD data, revealed that the denatured state becomes more compact in the presence of glucose. With no change in exposure of the native or transition state to solvent in crowded solutions, this would decrease the value of m_{k_F} sufficiently to lower the β_T-value. It is likely that the decrease in β_T observed by Russo and coworkers for FKBP12 [30] is also caused by changes in exposure of the denatured state. A wider investigation into the behaviour of the transition state of other two-state folders in crowded environments should reveal whether apparent increases in the exposure of the transition state are in fact caused by changes in exposure of the denatured state, giving rise to decreased β_T-values in crowded solutions.

Why the remarkable conservation of the hydrophobic core of ubiquitin? Amongst the more likely reasons for conservation are increased misfolding, aggregation, degradation and a loss of the recognition surface of ubiquitin. We have addressed some of these possibilities in this study and there was no evidence for any aggregation under crowding conditions, nor did they suggest misfolding of the protein. All but one known hydrophobic core mutations destabilise ubiquitin without changing the fold of the protein [1], making changes in the recognition surface of ubiquitin unlikely. This leaves decreased stability and, therefore, increased rates of degradation of ubiquitin as the most likely reason for conservation of the hydrophobic core. This hypothesis is currently under investigation (A. Roberts and S. E. Jackson, unpublished results).

Ubiquitin is involved in targeting proteins to the 26S proteasome for destruction [2–5], and is actually degraded by the proteasome with a half-life of 2 h in yeast [64]. The rate of degradation of proteins is linked to their thermodynamic stability because they must be unfolded to enter the cavity in the proteasome where the protein is degraded [65,66]. The majority of even conservative hydrophobic mutations, however, destabilise ubiquitin by over 2 kcal/mol *in vitro* [12], suggesting that they could be degraded significantly quicker to deplete ubiquitin pools below levels required for tolerance to a host of environmental stresses [7] and inhibit sexual reproduction [67].

The studies in this paper show that the relative stability difference between ubiquitin mutants in dilute and crowded solutions remains the same. Hydrophobic core mutations would therefore seriously disadvantage any organism experiencing stressful conditions, with purifying evolutionary selection [68] favouring those containing wild-type ubiquitin. We therefore have a reasonable hypothesis for ubiquitin's remarkable sequence conservation based on the same absolute increase in stability occurring for both wild-type and mutant ubiquitin under crowding conditions.

References

[1] S.E. Jackson, Ubiquitin: a small protein folding paradigm, Org. Biomol. Chem. 4 (10) (2006) 1845–1853.
[2] M. Hochstrasser, Ubiquitin-dependent protein degradation, Annu. Rev. Genet. 30 (1996) 405–439.
[3] A.M. Weissman, Regulating protein degradation by ubiquitination, Immunol. Today 18 (4) (1997) 189–198.
[4] J.S. Bonifacino, A.M. Weissman, Ubiquitin and the control of protein fate in the secretory and endocytic pathways, Annu. Rev. Cell. Dev. Biol. 14 (1998) 19–57.
[5] A. Hershko, A. Ciechanover, The ubiquitin system, Annu. Rev. Biochem. 67 (1998) 425–479.
[6] K.E. Sloper-Mould, J.C. Jemc, C.M. Pickart, L. Hicke, Distinct functional surface regions on ubiquitin, J. Biol. Chem. 276 (32) (2001) 30483–30489.
[7] D. Finley, E. Ozkaynak, A. Varshavsky, The yeast polyubiquitin gene is essential for resistance to high temperatures, starvation, and other stresses, Cell 48 (1987) 1035–1046.
[8] J.R. Simon, J.M. Treger, K. McEntee, Multiple independent regulatory pathways control ubi4 expression after heat shock in *Saccharomyces cerevisiae*, Mol. Microbiol. 31 (3) (1999) 823–832.
[9] D.J. Ecker, T.R. Butt, J. Marsh, E.J. Sternberg, N. Margolis, B.P. Monia, S. Jonnalagadda, M.I. Khan, P.L. Weber, L. Mueller, et al., Gene synthesis, expression, structures, and functional activities of site-specific mutants of ubiquitin, J. Biol. Chem. 262 (29) (1987) 14213–14221.
[10] M.D. Finucane, D.N. Woolfson, Core-directed protein design. II. Rescue of a multiply mutated and destabilized variant of ubiquitin, Biochemistry 38 (36) (1999) 11613–11623.
[11] C.G. Benitez-Cardoza, K. Stott, M. Hirshberg, H.M. Went, D.N. Woolfson, S.E. Jackson, Exploring sequence/folding space: folding studies on multiple hydrophobic core mutants of ubiquitin, Biochemistry 43 (18) (2004) 5195–5203.
[12] H.M. Went, S.E. Jackson, Ubiquitin folds through a highly polarized transition state, Protein Eng. Des. Sel. 18 (5) (2005) 229–237.
[13] Z. Ignatova, L.M. Gierasch, Monitoring protein stability and aggregation in vivo by real-time fluorescent labeling, PNAS 101 (2) (2004) 523–528.
[14] Z. Ignatova, L.M. Gierasch, Inhibition of protein aggregation in vitro and in vivo by a natural osmoprotectant, PNAS.
[15] S. Oas, T.G. Ghaemmaghami, Quantitative stability measurement in vivo, Nat. Struct. Biol. 8 (10) (2001) 879–882.
[16] P.R. Davis-Searles, A.S. Morar, A.J. Saunders, D.A. Erie, G.J. Pielak, Sugar-induced molten-globule model, Biochemistry 37 (48) (1998) 17048–17053.
[17] M. Jourdan, M.S. Searle, Insights into the stability of native and partially folded states of ubiquitin: effects of cosolvents and denaturants on the thermodynamics of protein folding, Biochemistry 40 (34) (2001) 10317–10325.
[18] Y.-S. Kim, L.S. Jones, A. Dong, B.S. Kendrick, B.S. Chang, M.C. Manning, T.W. Randolph, J.F. Carpenter, Effects of sucrose on conformational equilibria and fluctuations within the native-state ensemble of proteins, Protein Sci. 12 (6) (2003) 1252–1261.

[19] Y.X. Qu, D.W. Bolen, Efficacy of macromolecular crowding in forcing proteins to fold, Biophys. Chem. 101 (2002) 155–165.
[20] A.G. Ladurner, A.R. Fersht, Upper limit of the time scale for diffusion and chain collapse in chymotrypsin inhibitor 2, Nat. Struct. Biol. 6 (1) (1999) 28–31.
[21] A.J. Saunders, P.R. Davis-Searles, D.L. Allen, G.J. Pielak, D.A. Erie, Osmolyte-induced changes in protein conformation equilibria, Biopolymers 53 (4) (2000) 293–307.
[22] K. Sasahara, P. McPhie, A.P. Minton, Effect of dextran on protein stability and conformation attributed to macromolecular crowding, J. Mol. Biol. 326 (2003) 1227–1237.
[23] A.P. Minton, Effect of a concentrated "inert" macromolecular cosolute on the stability of a globular protein with respect to denaturation by heat and by chaotropes: a statistical–thermodynamic model, Biophys. J. 78 (1) (2000) 101–109.
[24] Y.F. Liu, D.W. Bolen, The peptide backbone plays a dominant role in protein stabilization by naturally-occurring osmolytes, Biochemistry 34 (39) (1995) 12884–12891.
[25] Y.X. Qu, C.L. Bolen, D.W. Bolen, Osmolyte-driven contraction of a random coil protein, PNAS 95 (16) (1998) 9268–9273.
[26] M. Auton, D.W. Bolen, Additive transfer free energies of the peptide backbone unit that are independent of the model compound and the choice of concentration scale, Biochemistry 43 (5) (2004) 1329–1342.
[27] M. Auton, D.W. Bolen, Predicting the energetics of osmolyte-induced protein folding/unfolding, PNAS 102 (42) (2005) 15065–15068.
[28] R.J. Ellis, Macromolecular crowding: an important but neglected aspect of the intracellular environment, Curr. Opin. Struct. Biol. 11 (1) (2001) 114–119.
[29] M. Silow, M. Oliveberg, High concentrations of viscogens decrease the protein folding rate constant by prematurely collapsing the coil, J. Mol. Biol. 326 (1) (2003) 263–271.
[30] A.T. Russo, J. Rosgen, D.W. Bolen, Osmolyte effects on kinetics of fkbp12 c22a folding coupled with prolyl isomerization, J. Mol. Biol. 330 (4) (2003) 851–866.
[31] A.P. Minton, Implications of macromolecular crowding for protein assembly, Curr. Opin. Struct. Biol. 10 (1) (2000) 34–39.
[32] T. Kiefhaber, H.H. Kohler, F.X. Schmid, Kinetic coupling between protein folding and prolyl isomerization, J. Mol. Biol. 224 (1) (1992) 217–229.
[33] H.M. Went, C.G. Benitez-Cardoza, S.E. Jackson, Is an intermediate state populated on the folding pathway of ubiquitin? FEBS Lett. 567 (2–3) (2004) 333–338.
[34] E.R. Main, K.F. Fulton, S.E. Jackson, Folding pathway of fkbp12 and characterisation of the transition state, J. Mol. Biol. 291 (2) (1999) 429–444.
[35] S. Khorasanizadeh, I.D. Peters, T.R. Butt, H. Roder, Folding and stability of a tryptophan-containing mutant of ubiquitin, Biochemistry 32 (27) (1993) 7054–7063.
[36] S. Khorasanizadeh, I.D. Peters, H. Roder, Evidence for a three-state model of protein folding from kinetic analysis of ubiquitin variants with altered core residues, Nat. Struct. Biol. 3 (2) (1996) 193–205.
[37] H. Went, PhD thesis: Protein folding and assembly pathways, Ph.D. thesis, University of Cambridge (2002).
[38] B.A. Krantz, T.R. Sosnick, Distinguishing between two-state and three-state models for ubiquitin folding, Biochemistry 39 (38) (2000) 11696–11701.
[39] M.D. Crespo, E.R. Simpson, M.S. Searle, Population of on-pathway intermediates in the folding of ubiquitin, J. Mol. Biol. 360 (5) (2006) 1053–1066.
[40] S.E. Jackson, A.R. Fersht, Folding of chymotrypsin inhibitor 2. 1. Evidence for a two-state transition, Biochemistry 30 (43) (1991) 10428–10435.
[41] A.R. Fersht, Structure and Mechanism in Protein Science: A Guide to Enzyme Catalysis and Protein Folding, 4th Edition, W.H. Freeman and Company, 1998.
[42] A.R. Fersht, Chapter 17: Protein stability, Structure and mechanism in protein science: a guide to enzyme catalysis and protein folding, 4th Edition, W.H. Freeman and Company, 1998.
[43] M. Gerstein, A resolution-sensitive procedure for comparing protein surfaces and its application to the comparison of antigen-combining sites, Acta Crystallogr., A 48 (3) (1992) 271.
[44] G.I. Makhatadze, M.M. Lopez, J.M. Richardson, S.T. Thomas, Anion binding to the ubiquitin molecule, Protein Sci. 7 (3) (1998) 689–697.
[45] S.N. Timasheff, The control of protein stability and association by weak interactions with water: how do solvents affect these processes? Annu. Rev. Biophys. Biomol. Struct. 22 (1993) 67–97.
[46] T.P. Creamer, R. Srinivasan, G.D. Rose, Modeling unfolded states of peptides and proteins, Biochemistry 34 (50) (1995) 16245–16250.
[47] S. Miller, J. Janin, A.M. Lesk, C. Chothia, Interior and surface of monomeric proteins, J. Mol. Biol. 196 (3) (1987) 641–656.
[48] R. Beal, Q. Deveraux, G. Xia, M. Rechsteiner, C. Pickart, Surface hydrophobic residues of multiubiquitin chains essential for proteolytic targeting, PNAS 93 (2) (1996) 861–866.
[49] C.M. Pickart, D. Fushman, Polyubiquitin chains: polymeric protein signals, Curr. Opin. Chem. Biol. 8 (6) (2004) 610–616.
[50] D.J. Felitsky, J.G. Cannon, M.W. Capp, J. Hong, A.W. Van Wynsberghe, C.F. Anderson, J. Record, M.T., The exclusion of glycine betaine from anionic biopolymer surface: why glycine betaine is an effective osmoprotectant but also a compatible solute, Biochemistry 43 (46) (2004) 14732–14743.
[51] A.P. Minton, Influence of excluded volume upon macromolecular structure and associations in 'crowded' media, Curr. Opin. Biotechnol. 8 (1997) 65–69.
[52] A. Matouschek, D.E. Otzen, L.S. Itzhaki, S.E. Jackson, A.R. Fersht, Movement of the position of the transition state in protein folding, Biochemistry 34 (41) (1995) 13656–13662.
[53] D. Farcasiu, The use and misuse of the Hammond postulate, J. Chem. Ed. 52 (1975) 76–79.
[54] J.E. Leffler, E. Grunwald, Rates and Equilibria of Organic Reactions, Dover, New York, 1963.
[55] I.E. Sanchez, T. Kiefhaber, Hammond behavior versus ground state effects in protein folding: evidence for narrow free energy barriers and residual structure in unfolded states, J. Mol. Biol. 327 (4) (2003) 867–884.
[56] B.A. Krantz, R.S. Dothager, T.R. Sosnick, Discerning the structure and energy of multiple transition states in protein folding using psi-analysis, J. Mol. Biol. 337 (2) (2004) 463–475.
[57] N. Tokuriki, M. Kinjo, S. Negi, M. Hoshino, Y. Goto, I. Urabe, T. Yomo, Protein folding by the effects of macromolecular crowding, Protein Sci. 13 (1) (2004) 125–133.
[58] A. Almagor, A. Priev, G. Barshtein, B. Gavish, S. Yedgar, Reduction of protein volume and compressibility by macromolecular cosolvents: dependence on the cosolvent molecular weight, Biochim. Biophys. Acta (BBA) — Protein Struct. Mol. Enzymol. 1382 (1) (1998) 151–156.
[59] J. Jacob, B. Krantz, R.S. Dothager, P. Thiyagarajan, T.R. Sosnick, Early collapse is not an obligate step in protein folding, J. Mol. Biol. 338 (2) (2004) 369–382.
[60] D.S. Spencer, K. Xu, T.M. Logan, H.X. Zhou, Effects of pH, salt, and macromolecular crowding on the stability of fk506-binding protein: an integrated experimental and theoretical study, J. Mol. Biol. 351 (1) (2005) 219–232.
[61] B. van den Berg, R.J. Ellis, C.M. Dobson, Effects of macromolecular crowding on protein folding and aggregation, EMBO J. 18 (24) (1999) 6927–6933.
[62] B.R. Zhou, Y. Liang, F. Du, Z. Zhou, J. Chen, Mixed macromolecular crowding accelerates the oxidative refolding of reduced, denatured lysozyme, J. Biol. Chem. 279 (53) (2004) 55109–55116.
[63] D. Hall, A.P. Minton, Macromolecular crowding: qualitative and semiquantitative successes, quantitative challenges, Biochim. Biophys. Acta (BBA) — Proteins Proteomics 1649 (2) (2003) 127–139.
[64] J. Hanna, D.S. Leggett, D. Finley, Ubiquitin depletion as a key mediator of toxicity by translational inhibitors, Mol. Cell. Biol. 23 (24) (2003) 9251–9261.
[65] M.M. Garcia-Alai, M. Gallo, M. Salame, D.E. Wetzler, A.A. McBride, M. Paci, D.O. Cicero, G. de Prat-Gay, Molecular basis for phosphorylation-dependent, pest-mediated protein turnover, Structure 14 (2) (2006) 309–319.
[66] C. Lee, M.P. Schwartz, S. Prakash, M. Iwakura, A. Matouschek, Atp-dependent proteases degrade their substrates by processively unraveling them from the degradation signal, Mol. Cell 7 (3) (2001) 627–637.
[67] K. Okazaki, H. Okayama, O. Niwa, The polyubiquitin gene is essential for meiosis in fission yeast, Exp. Cell. Res. 254 (1) (2000) 143–152.
[68] M. Nei, I.B. Rogozin, H. Piontkivska, Purifying selection and birth-and-death evolution in the ubiquitin gene family, PNAS 97 (20) (2000) 10866–10871.